

# RSC Advances



This is an *Accepted Manuscript*, which has been through the Royal Society of Chemistry peer review process and has been accepted for publication.

*Accepted Manuscripts* are published online shortly after acceptance, before technical editing, formatting and proof reading. Using this free service, authors can make their results available to the community, in citable form, before we publish the edited article. This *Accepted Manuscript* will be replaced by the edited, formatted and paginated article as soon as this is available.

You can find more information about *Accepted Manuscripts* in the [Information for Authors](#).

Please note that technical editing may introduce minor changes to the text and/or graphics, which may alter content. The journal's standard [Terms & Conditions](#) and the [Ethical guidelines](#) still apply. In no event shall the Royal Society of Chemistry be held responsible for any errors or omissions in this *Accepted Manuscript* or any consequences arising from the use of any information it contains.

**Study of post separation pH adjustment by microchip for analysis of aminoglycoside antibiotics**

Xiangying Meng<sup>1</sup>, Xingmei Suo<sup>2</sup>, Beiyuan Fan<sup>1</sup>, Yongliang Yu<sup>3</sup>, Yongsheng Ding<sup>1\*</sup>

Affiliation:

1 College of Life Sciences, University of Chinese Academy of Sciences, Beijing 100049, China

2 School of Information Engineering, Minzu University of China, Beijing 100081, China

3 School of Physics, University of Chinese Academy of Sciences, Beijing 100049, China

\*Corresponding author: Dr. Yongsheng Ding

Postal address: College of Life Sciences, University of Chinese Academy of Sciences

19A Yuquanlu Road, Beijing 100049, China

Phone: 86-10-88256392

Fax: 86-10-88256079

Email: dingysh@ucas.ac.cn

**ABSTRACT**

Recently, we have developed a simple microchip to simultaneously accommodate acidic condition for separation and alkaline condition for electrochemical detection of aminoglycoside antibiotics [Electrophoresis, DOI: 10.1002/elps.201200309]. With two branch channels connected near to the end of separation channel, alkaline solution was hydrostatically introduced into a Z-shape mixing channel and combined with acidic stream from separation channel. As a result, the pH of mixed solution was adjusted to the desired value for electrochemical detection of aminoglycoside antibiotics. In this manuscript, the principle and related parameters of the pH adjustment on the microchip were investigated both in theory and practice. With the guidance of the principle of the post separation pH adjustment, we applied the functional microchip for analysis of six aminoglycoside antibiotics in biological sample with the satisfied analytical performances. Specifically, these compounds were electrophoretically separated under 5 mM sodium acetate (pH = 4) and 0.6 mM CTAB, and through the post separation pH adjustment, electrochemically detected in alkaline condition (pH > 12) at a Cu-Sn-Cr alloy electrode. Additionally, this microchip may provide possible use of post separation reagent addition for enzyme-assisted electrochemical detection.

Key words: post separation pH adjustment; aminoglycoside antibiotics; alloy electrode; microchip

## INTRODUCTION

Aminoglycosides (AMGs) are effective drugs that are widely used in therapy against bacterial infections, but their clinical use has been restricted due to toxic side effects, especially to the kidneys and the ear. On the other hand, low cost means that they are often widely used in animal husbandry leading to potential residues in the food chain, which probably increase the bacterial resistance against AMG antibiotics in human body. Since these compounds are characterized by two or more amino sugars linked by glycosidic bonds to an aminocyclitol component, in general, they are short of chromophores and show high polarity. Due to these reasons, the detection of AMGs using standard HPLC or GC instrumentation generally requires the pre- or post-column derivatization<sup>1-5</sup>. Besides these derivatization methods, electrochemical detection is usually coupled with chromatographic techniques for the determination of AMGs without derivatization. However, in most cases, the use of electrochemical detection for analysis of carbohydrates requires strongly alkaline condition ( $\text{pH} > 12$ ), which is unfavorable to the separation of AMGs by CE or non ionic exchanger column<sup>6-9</sup>. Although the methods based on LC-MS/MS are most powerful for screening and confirmation of AMGs, they are high cost to operate and require highly qualified personnel<sup>10-13</sup>. Consequently, the necessity still exists for rapid, facile, and low cost screening methods both in the laboratory and at onsite locations. Up to now, a few methods of screening AMGs have been reported with relatively high sensitivity, such as the surface plasmon resonance (SPR)-based biosensors<sup>14</sup> and aptamer-based sensors<sup>15,16</sup>. However, most of them depend on cost antibodies or RNA aptamers without the separation of multiple drugs.

Microfluidic technology has evolved over the past two decades, accompanying a wealth of

inventions and applications which have extensively attracted attentions from a variety of scientific communities. The recent achievements and applications of microfluidic technology have been well documented in several review articles<sup>17-20</sup>. Distinctively, the microchip coupled with electrochemical detection shows several merits, such as miniaturization of analytical systems and simplicity for use. Recently, we have developed a simple microfluidic chip containing two branch channels connected to the separation channel nearby the detection point, in which the alkaline solutions conflux with the acidic stream toward an alloy modified electrode for electrochemical detection of AMGs<sup>21</sup>. To better take advantage of this microchip, here we did further studies on the post separation pH adjustment both in theory and practice. In addition, the electroplating conditions of the alloy electrode were reinvestigated to improve the stability of the electrode. The experiments show the microchip with re-modified electrode can be kept in use for more than a week. The applicability of the method has been demonstrated by analyzing six aminoglycoside antibiotics in bovine serum sample. Such a straightforward approach is a prototype of “post-column” addition based on microfluidic platform and also properly applied to other post separation adjustment or reaction with various reagents (e.g. enzymes) to accommodate the separation and detection in the different conditions.

## **EXPERIMENTAL SECTION**

### **Chemicals and Solutions**

SU-8 2035 photoresist and SU-8 developer were purchased from MicroChem (Newton, MA, USA). Sylgard 184 silicone elastomer and curing agent were obtained from Dow Corning (Midland, MI, USA). Cetyltrimethyl ammonium bromide (CTAB) was purchased from

Sigma-Aldrich (Shanghai, China). Analytical grade sodium acetate, copper sulfate, tin chloride, chromium chloride, acetic acid, sulfuric acid, hydrochloric acid, and sodium hydroxide were obtained from Beijing Chemical Reagent Company (Beijing, China) and used without further purification. The six AMG standards, spectinomycin (SPE), streptomycin (STR), amikacin (AMI), kanamycin A (KAN A), paromomycin (PAR), and neomycin (NEO), were obtained from National Institutes for Food and Drug Control (China). Running buffers were prepared by diluting the stock solutions of sodium acetate and CTAB with deionized water to the desired concentrations. The pH of the buffer solution was adjusted by small additions of either 0.1M NaOH or 0.1M HCl. The stock solutions of AMG antibiotics were prepared in distilled water and diluted with the running buffer. All aqueous solutions were prepared using 18.2 M $\Omega$ -cm resistance water (Elga Labwater, UK) and were stored at 4 °C when not in use.

#### **Fabrication of the Microfluidic Chip**

The fabrication of the microfluidic chips was performed as described elsewhere<sup>22, 23</sup>. Briefly, a 100 mm diameter silicon wafer (Tianjin Semiconductor Institute of Technology, Tianjin, China) was cleaned with piranha solution (3 parts of 98 % H<sub>2</sub>SO<sub>4</sub> with 1 part of 30 % H<sub>2</sub>O<sub>2</sub>; **CAUTION:** piranha solution is a powerful oxidizing agent that reacts violently with organic compounds and should be handled with extreme care) and thoroughly rinsed with deionized water. The wafer was then dried at 200 °C for 30 min. Next, the wafer was coated with SU-8 2035 negative photoresist using a spin coater (Laurell Technologies, PA, USA) by dispensing approximate 3 ml of photoresist onto the wafer. A spread cycle of 500 rpm for 10 s followed by 1500 rpm for 30 s was performed followed by two pre-exposure baking steps at 65 and 95 °C for 5 and 30 min,

respectively. A digitally produced mask containing the channel pattern was placed on the coated wafer, exposed to light via a near-UV flood source (Optical Associates Inc., CA, USA) for 30 s and then followed by a post exposure baking sequence. The positive relief was developed by placing the wafer in SU-8 developer (propylene glycol methyl ether acetate) for 15 min, rinsing with isopropanol and drying under nitrogen stream. The height of the positive patterns on the molding master is equal to the channel depth created in the PDMS layer. It was measured roughly by cutting a piece of PDMS with cross section of the channel under a microscope with microscopic length scale. Two PDMS layers were fabricated by pouring a degassed mixture of Sylgard 184 silicone elastomer and curing agent (10:1) onto either a molding master or a blank wafer, followed by curing at 65 °C for at least 2 h. The cured PDMS was separated from the mold and reservoirs were made at the end of each channel using a 5-mm circular punch. A platinum wire coated with Cu-Sn-Cr alloy was then aligned at the end of the separation channel in a perpendicular channel designed for working electrode. Next, the two PDMS layers were placed in plasma cleaner (Harrick Plasma, NY, USA), oxidized for 30 s and immediately brought into conformal contact to form an irreversible seal. The extremities of the electrode channel were sealed with two drops of super glue. Finally, an electrical connection to the working electrode was made using silver paint (SPI Supplies, PA, USA) and a copper wire. A schematic drawing of the microfluidic chip is illustrated in Figure 1.

**Figure 1**

### **Instrumentation**

A high voltage sequencer (LabSmith Inc., CA, USA), with an adjustable voltage range of – 3000 to + 3000 V, was used for all of the electrophoresis experiments. Before the experiments, the

microchannels were preconditioned by sequentially rinsing them with 0.1 M NaOH, deionized water and running buffer. The microfluidic chip and the operation were described in detail as follows. The separation channel was 57 mm long. A double-T injector, with a 500  $\mu\text{m}$  gap between side channels and defining a 1.2 nL sample plug, was used for all experiments. The amount of buffer dispensed in each reservoir (RB, S, SW and BW) was 60  $\mu\text{l}$ , except for two alkaline solution reservoirs (A1 and A2) where 120  $\mu\text{L}$  of 0.3 M NaOH were dispensed in order to hydrostatically push the alkaline solution into the mixing channel. The solution in each reservoir was refreshed after 5 to 6 run times in consideration of evaporation. The 2-mm length mixing channel was designed as Z - shape to aggrandize mix of solution. During the sample injection, the potentials of  $-400\text{ V}$  and  $+100\text{ V}$  were applied to the reservoirs S and SW, respectively, while the reservoir RB was floating. During the separation step, the reservoir RB was applied to  $-1000\text{ V}$ , at mean time, the reservoirs S and SW were floating. During the above proceedings, the waste reservoir (BW) was always grounded. The present design allows the isolation of the detector from the separation current through the end-column configuration. Electrical connections were made to the microfluidic devices with platinum electrodes placed into the reservoirs at the ends of each channel (except for the reservoirs A1 and A2). Electrochemical experiments were performed with a CHI 810 C (Chenghua Instruments Co., Shanghai, China), using a three-electrode setup. An Ag / AgCl (3.0 M KCl) reference electrode and a platinum wire were used as the reference and auxiliary electrodes, respectively. A 5-cm length platinum wire (25- $\mu\text{m}$  diameter) was used as the substrate electrode (effective length = 3 cm), on which the electrodeposition was carried out at  $-0.3\text{ V}$  (vs. Ag / AgCl) for 150 s in an electroplating bath containing 50 mM  $\text{CuSO}_4$ , 0.2 mM  $\text{SnCl}_2$ , 1.0 mM  $\text{CrCl}_3$ , 2.0 mM EDTA and 10 mM  $\text{H}_2\text{SO}_4$ . The coated electrodes were also applied for

cyclic voltammetry and amperometric i-t curve experiments.

### Sample preparation

0.5 mL bovine serums were spiked with AG antibiotics at three concentration levels (20  $\mu$ M, 50  $\mu$ M and 100  $\mu$ M), vortexed with 0.5 mL TCA (20% (w/v)), ultrasonicated for 10 min, and then centrifuged at 12,000 rpm for 10 min. After removing the protein sediment, the supernatant was transferred to another centrifuge tube, and then added EDTA to 10 mM. The extraction of AMGs in the solution was conducted using a solid phase extraction (SPE) column (Anpelclean MCX, 60 mg, Shanghai, China). The SPE procedures were detailed as follows: loading the solution on the preconditioned column at a flow rate of 0.2 mL/min, then washing with water until the effluent was neutral solution, finally eluting with 6 mL of 10% (v/v) ammonia in methanol at a flow rate of 0.2 mL/min. The collected eluent was evaporated under a nitrogen stream in water bath at 60 °C and the residue was reconstituted in 0.5 mL of the running buffer for injection.

## RESULTS AND DISCUSSION

### Theoretical Description of Post Separation Adjustment of pH

To better understand the behavior of the post separation adjustment of pH based on our designed microchip, the theoretical study was described below. For a laminar flow governed by Poiseuille equation, the volumetric flow rate is proportional to the pressure difference and the forth power radius of the channel while inversely proportional to the viscosity and the length of channel. The equation is given as follow:

$$Q = \pi \Delta P r^4 / (8 \mu L) \quad (1)$$

where  $Q$  is the volumetric flow rate;  $\Delta P$  is the pressure drop;  $L$  is the length of channel;  $\mu$  is the viscosity of fluid;  $r$  is the radius of channel;  $\pi$  is the mathematical constant Pi. During the separation step, the pH of the mixed solution arriving at the detection electrode depends on the amount of alkaline solution flowing into the Z-shape mixing channel, which is controlled by the pressure drop between the reservoirs A1 / A2 and BW. In this microchip, the pressure drop is deduced from the difference between the height of the solution in the reservoir A1 / A2 and BW.

$$\Delta P = \rho g (h_A - h_{BW}) \quad (2)$$

where  $\rho$  is the density of water,  $g$  is gravity constant,  $h_A$  and  $h_{BW}$  are the heights of solution in the reservoir A1 / A2 and BW.

For a cylinder-like reservoir of the microfluidic chip,

$$h = V / \pi R^2 \quad (3)$$

where  $h$  is the height of solution in reservoir,  $V$  is the volume of solution in reservoir,  $R$  is the radius of reservoir.

Combining the equations (1), (2) and (3), the Poiseuille equation governing the flow rate of the solution in the branch channels of the microchip can be written as follow:

$$Q_b = \rho g (V_A - V_{BW}) r^4 / (8\mu L R^2) \quad (4)$$

where  $Q_b$  is the volumetric flow rate in the branch channel,  $V_A$  and  $V_{BW}$  are the volume of solution in the reservoir A1 / A2 and BW, respectively. For the post separation adjustment of pH in this experiment, the alkaline solutions in the reservoirs A1 and A2 start to flow into the mixing channel when the pressure drop is formed between the reservoir A and BW ( $V_A - V_{BW} > 0$ ). In order to sustain an appropriate and steady pH value for the electrochemical detection, a hydrodynamic equilibrium is required to form in the mixing channel, where an active electroosmotic flow (EOF)

from the upstream separation channel combines two hydrostatically driven flows from the branch channels toward the detection point. With mixing thoroughly, the pH of the mixed solution at the detection point can be calculated by the following equation:

$$\text{pH} = 14 + \lg [2 C_{\text{NaOH}} Q_b / (Q_m + 2 Q_b)] \quad (5)$$

where  $Q_m$  is the volumetric flow rate of EOF in the upstream separation channel,  $C_{\text{NaOH}}$  is the concentration of NaOH applied in the reservoirs A1 and A2. Because the volumetric flow rate from the separation channel is determined by the EOF,  $Q_m$  can be obtained from the following equation:

$$Q_m = \pi r^2 v_{\text{eof}} \quad (6)$$

where  $v_{\text{eof}}$  is the velocity of EOF. In this experiment, the actual value of EOF is about 1.0 mm / s at - 1000V of the separation potential.

Combining the equation (4), (5) and (6), the pH of the mixed solution at the end of separation channel can be approximately calculated according to the volume difference between the reservoirs A and BW and the concentration of NaOH in the reservoirs A. Under the certain velocity of EOF and the given concentration of NaOH, a series of theoretical curves between the pH and the volume difference ( $V_A - V_{\text{BW}}$ ) are plotted in Figure 2A. All of the plots show the same tendency that the pH of the mixed solution increases steeply during the volume difference ( $V_A - V_{\text{BW}}$ ) initially increasing from 2.5 to 25  $\mu\text{L}$ , then the increment of pH becomes relatively flat when the volume difference is larger than 25  $\mu\text{L}$ . However, when the larger volume difference is applied, the larger dilution percent formed is likely to decrease the response of analyte. The dilution percent can be defined as the following formula:

$$\text{Dilu. \%} = 100 \times Q_m / (Q_m + 2Q_b) \quad (7)$$

Additionally, we apply Comsol 3.2 (student version) software to simulate the pH distribution in the mixing channel and virtually estimate the pH of the solution surrounding the detection point. Figure 2B shows that the designed microchip can generate a high pH nearby the detection point under the given conditions of  $Q_b = 0.1 \times Q_m$  and  $C_{\text{NaOH}} = 0.1 \text{ M}$ .

**Figure 2**

### **Experimental Verification of Post Separation Adjustment of pH**

With the guidance from the above theoretical descriptions, the effect of the different concentration of NaOH in the reservoir A (1 / 2) and volume difference of solution ( $V_{A-BW}$ ) on the response of AMGs were investigated. Figure 3A shows the electrochemical responses of the analytes under the different concentrations of NaOH at a constant volume difference (60  $\mu\text{L}$ ). Compared to 0.1 M and 0.5 M NaOH, the peak currents of the analytes were largest under 0.3 M NaOH. It was in part consistent with the higher concentration of NaOH leading to the higher pH to facilitate the electrochemical oxidization of AMG. On the other hand, the peak currents of the AMGs under 0.5 M NaOH were smaller than those under 0.3 M NaOH. It can be explained the excessively high pH over 13 results in the high background current to diminish the peak currents of AMGs. Thus, 0.3 M NaOH was selected in the following experiments. In order to obtain the larger and more stable peak currents of analytes, the percent of dilution and optimal pH need to be balanced at a certain concentration of NaOH. For the given concentration of NaOH, the choosing of larger volume difference means that more alkaline solution flows into the mixing channel resulting larger percent of dilution and higher pH, whereas applying lower volume difference results lower pH and dilution. The effect of the volume difference under 0.3 M NaOH on the electrochemical response of AMGs was given in Figure 3B. At the volume difference of 60  $\mu\text{L}$ , the peak currents were

largest obviously. This phenomenon is well in accordance with larger volume difference resulting larger dilution percent and smaller volume difference resulting lower pH. Finally, 60  $\mu\text{L}$  was selected as the optimal volume difference in the following experiments. The above experimental results show clear evidence for the theoretical descriptions.

**Figure 3**

### **Electrochemical Characters of the Alloy Working Electrode**

Electrochemical detections of carbohydrates have extensively been studied at different metal electrodes. Conclusively, pulsed electrochemical detection (PED) needs to be applied on noble metal electrode (e.g. Au and Pt)<sup>24,25</sup>, while constant potential amperometry needs to be applied on copper or nickel electrode<sup>26,27</sup>. However, both detection modes need metallic oxide catalysis under strongly alkaline condition (generally  $\text{pH} > 12$ ). In our preliminary study, both of gold and copper wires were adopted as the working electrode for PED and constant potential amperometry, respectively. However, the unavoidable hindrances were incurred during applying detection potential on these electrodes, such as low sensitivity, bubble formation on gold electrode or severe corrosion to copper electrode, etc. To overcome these problems, platinum wire was selected as a substrate, on which the multiple metal elements (Cu-Sn-Cr) were coelectrodeposited to form the distinctive nanostructures with the large ratio of surface-to-volume (Figure 4 A) and show the character of corrosion-resistant (at least use for one week). The electrochemical behaviors of the electrodeposited wire were characterized by conducting cyclic voltammetry (CV) and amperometric *i-t* experiments. As can be observed in Figure 4B, the CV data indicate an oxidative peak of AMI on the modified electrode came out when the pH increased from 11 to 13. The more details about the catalytically electrochemical oxidation of AMGs at copper based electrode were

discussed in our previous work<sup>21</sup>. On the other hand, amperometric i-t data in Figure 4C exhibit the alloy modified electrode providing an obviously large sensitivity compared to the copper and platinum electrode. The improvement of the sensitivity on the modified electrode is mainly due to the significant nanostructures formed on the alloy electrode.

#### Figure 4

#### The Separation of AMGs

The electrophoretic separation of the selected AMGs is likely to be obtained under acidic running buffer due to the protonation of their amino groups. However, the dissociation of silanols on inner surface of PDMS microchannel will be suppressed under acidic condition, thus the EOF become near to zero. To improve the separation, the CTAB is chosen to modify the surface of the separation channel through forming positively charged layer on the surface to reverse the direction of EOF. Under anodic mode, the reversed EOF is opposite to the direction of the electrophoretic mobility of positively charged analytes, leading to the relatively long migration time that is of benefit to the separation of AMGs. As can be seen in Figure 5A, the reversed EOF became constant when the CTAB concentrations were larger than 0.6 mM because of the saturation of CTAB absorption on the surface. The separation order of the selected AMGs depends on the number of amino groups in molecule. The longer migration time corresponds with the more amino groups while the shorter migration time is related to the less amino groups (the molecular structures of the six AMGs shown in Figure S-1 of the supporting information). The effect of the pH of the buffer on the separation depends on the degree of protonation of amino groups (shown in Figure 5B), when the pH was 5.0, the three peaks of AMGs (AMI, KAN A, and PAR) merged into a single peak. In contrast with decreasing the pH to 4.0, the baseline separation of six AMGs

was achieved within 5 min. Thus pH = 4.0 was selected as the optimal pH of the running buffer in this experiment. Generally, the higher separation voltage produces the larger EOF that makes migration time shorter and peak height larger. It was worth noting in Figure 5C that the peak currents of the AMGs became smaller with increasing the separation voltage; on the other hand, the noise became large obviously at – 800 V of the separation voltage. These phenomena can be explained that the higher separation voltages (e.g.– 1400 V) increased EOF and caused the larger volume of the acidic buffer flowing into the mixing channel to decrease the pH of the mixed solution resulting the smaller peak currents, whereas the lower separation voltage (e.g. – 800 V) decreased EOF and caused the larger volume of the alkaline solution from the branch channels flowing into the mixing channel and resulted in the larger noise at the higher pH condition. Finally, – 1000 V was selected as the optimal separation voltage. The effect of the concentrations of sodium acetate between 2.0 to 10 mM on the separation and detection was not obvious (the data not shown here). However, when the concentration of sodium acetate is larger than 10 mM, the bubbles are formed in the separation channel and the larger buffer capacity requires the more alkaline solution for pH adjustment. Thus, the concentration of sodium acetate was selected as 5 mM.

### Figure 5

#### Analytical Performances

Under the optimal conditions (combining 5.0 mM sodium acetate, pH = 4.0 and 0.6 mM CTAB as the running buffer, – 1000 V as the separation voltage, 60  $\mu$ L as the volume difference between the reservoir A and BW, 10 s as the injection time, and 0.65 V as the detection potential), the response of the detector was analyzed as function of the concentration for the six AMGs. The linear

relationships between concentration and peak current were obtained for SPE, STR, AMI, KAN A, PAR, and NEO at the range of 1.0 to 100  $\mu\text{M}$  with  $R^2 > 0.99$  and the limits of detection were between 0.2 to 2.0  $\mu\text{M}$  at a ratio of signal-to-noise of 3. In order to demonstrate the stability of the modified electrode, repetitive injections ( $n = 30$ ) were performed. The RSDs in peak current and migration time were less than 6.2 % and 3.0 %, respectively. Above analytical parameters (linear range, slope, correlation coefficient, LODs, and stability) for each analyte were summarized in Table S-1 of the supporting information. To further evaluate the accuracy and performance of the method, the recovery experiments under the optimum conditions were conducted with six AMGs spiked in serum samples at three concentration levels of 20  $\mu\text{M}$ , 50  $\mu\text{M}$  and 100  $\mu\text{M}$ . As can be seen in Figure 6, a standard mixture of the AMGs (curve a), a spiked serum sample (curve b), and a blank serum sample extract (curve c) were obtained under the optimum conditions. The average recoveries ( $n=3$ ) were  $84.2 \pm 4.1\%$ ,  $68.2 \pm 5.1\%$ ,  $73.6 \pm 3.9\%$ ,  $88.9 \pm 4.4\%$ ,  $86.2 \pm 4.2\%$  and  $79.6 \pm 4.9\%$  for SPE, STR, AMI, KAN A, PAR, and NEO, respectively.

**Figure 6**

## CONCLUSIONS

This manuscript described in detail the post separation pH adjustment on microchip and its utility of the analysis of AMGs. Specifically, the present methodology adjusted pH after the separation of AMGs under the acidic buffer and then applied the electrochemical detection of AMGs under the alkaline condition. With the optimized conditions, the six AMGs were baseline separated within 5 min and detected at the relatively low micromolar level. The method offers a simple, sensitive, and portable method for analysis of AMGs in biological sample without derivatization.

Additionally, this type of microchip provides a simple way for use of post separation reagent

addition for other applications.

#### **ACKNOWLEDGMENTS**

This project was supported by National Natural Sciences Foundation of China (21075135) and the Chinese Academy of Sciences (No.KSCX2-EW-J-29).

The authors declare no competing financial interest

## REFERENCES

1. M. Zhou, G. Wei, Y. Liu, Y. Sun, S. Xiao, L. Lu, C. Liu and D. Zhong, *J Chromatogr B Analyt Technol Biomed Life Sci*, 2003, **798**, 43-48.
2. P. Vinas, N. Balsalobre and M. Hernandez-Cordoba, *Talanta*, 2007, **72**, 808-812.
3. C. Z. Yu, Y. Z. He, G. N. Fu, H. Y. Xie and W. E. Gan, *J Chromatogr B Analyt Technol Biomed Life Sci*, 2009, **877**, 333-338.
4. D. A. Stead, *Journal of chromatography*, 2000, **747**, 69-93.
5. T. A. McGlinchey, P. A. Rafter, F. Regan and G. P. McMahon, *Analytica chimica acta*, 2008, **624**, 1-15.
6. P. D. Voegel and R. P. Baldwin, *Electroanalysis*, 1997, **9**, 1145-1151.
7. W. C. Yang, A. M. Yu and H. Y. Chen, *J. Chromatogr. A*, 2001, **905**, 309-318.
8. G. Brajanoski, J. Hoogmartens, K. Allegaert and E. Adams, *J. Chromatogr. B*, 2008, **867**, 149-152.
9. V. P. Hanco, J. S. Rohrer, H. H. Liu, C. Zheng, S. Zhang, X. Liu and X. Tang, *Journal of pharmaceutical and biomedical analysis*, 2008, **47**, 828-833.
10. D. A. Bohm, C. S. Stachel and P. Gowik, *Analytica chimica acta*, 2010, **672**, 103-106.
11. C. ChiaoChan, U. Koesukwiwat, S. Yudthavorasit and N. Leepipatpiboon, *Analytica chimica acta*, 2010, **682**, 117-129.
12. A. Kaufmann, P. Butcher and K. Maden, *Analytica chimica acta*, 2012, **711**, 46-53.
13. F. L. van Holthoon, M. L. Essers, P. J. Mulder, S. L. Stead, M. Caldow, H. M. Ashwin and M. Sharman, *Analytica chimica acta*, 2009, **637**, 135-143.
14. S. Rebe Raz, M. G. E. G. Bremer, W. Haasnoot and W. Norde, *Analytical Chemistry*, 2009, **81**, 7743-7749.
15. A. A. Rowe, E. A. Miller and K. W. Plaxco, *Analytical Chemistry*, 2010, **82**, 7090-7095.
16. N. Derbyshire, S. J. White, D. H. J. Bunka, L. Song, S. Stead, J. Tarbin, M. Sharman, D. Zhou and P. G. Stockley, *Analytical Chemistry*, 2012, **84**, 6595-6602.
17. D. Gao, H. Liu, Y. Jiang and J.-M. Lin, *Lab on a chip*, 2013, **13**, 3309-3322.
18. E. Primiceri, M. S. Chiriaco, R. Rinaldi and G. Maruccio, *Lab on a chip*, 2013, **13**, 3789-3802.
19. B.-B. Xu, Y.-L. Zhang, H. Xia, W.-F. Dong, H. Ding and H.-B. Sun, *Lab on a chip*, 2013, **13**, 1677-1690.
20. L. Yu, S. R. Ng, Y. Xu, H. Dong, Y. J. Wang and C. M. Li, *Lab on a chip*, 2013, **13**, 3163-3182.
21. Y. Ding, L. Bai, X. Suo and X. Meng, *Electrophoresis*, 2012, **33**, 3245-3253.
22. C. D. Garcia and C. S. Henry, *Anal Chem*, 2003, **75**, 4778-4783.
23. Y. Ding, A. Ayon and C. D. Garcia, *Analytica chimica acta*, 2007, **584**, 244-251.
24. G. Brajanoski, J. Hoogmartens, K. Allegaert and E. Adams, *J Chromatogr B Analyt Technol Biomed Life Sci*, 2008, **867**, 149-152.
25. V. Manyanga, K. Kreft, B. Divjak, J. Hoogmartens and E. Adams, *J Chromatogr A*, 2008, **1189**, 347-354.
26. F. Cao, S. Guo, H. Ma, G. Yang, S. Yang and J. Gong, *Talanta*, 2011, **86**, 214-220.
27. X. Zhang, A. Gu, G. Wang, Y. Huang, H. Ji and B. Fang, *The Analyst*, 2011, **136**, 5175-5180.

The list of the figure captions

Figure 1. The scheme and photography of the microfluidic chip. Channels: 50  $\mu\text{m}$  wide, 50  $\mu\text{m}$  deep. Injector (double-T) volume: 1.2 nL, separation channel: 57 mm, total length of Z-shape mixing channel: 2 mm, each double-T arms: 5 mm, each branch-like channel: 8 mm. Solution reservoirs: RB, running buffer reservoir; S, sample reservoir; SW, sample waste reservoir; BW, buffer waste reservoir; A1 / A2, alkaline reservoirs.

Figure 2. The plots (A) of the pH of the mixed solution vs. the volume difference (down x-axis) and the dilution percent of analytes (up x-axis); a computational simulation of the pH distribution in the mixing channel (B).

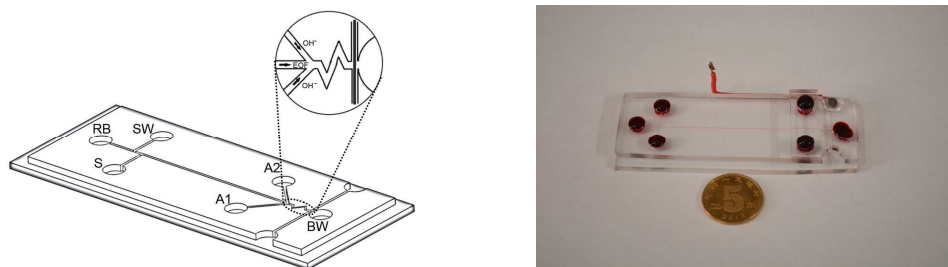
Figure 3. Electrophoregrams of AMGs under the post separation pH adjustment with the different concentration of NaOH at  $V_{(A-BW)} = 60 \mu\text{L}$  (A) and with the different  $V_{(A-BW)}$  at 0.3 M NaOH (B). Other conditions: running buffer 5 mM sodium acetate (pH = 4) with 0.6 mM CTAB, separation voltage – 1000 V, injection at -100 V / + 400 V for 10 s, detection potential = 0.65 V. The peak of the analytes (50  $\mu\text{M}$  each): 1 = SPE, 2 = STR, 3 = AMI, 4 = KAN A, 5 = PAR, 6 = NEO.

Figure 4. Characters of the alloy modified electrode: SEM of Cu-Sn-Cr alloy coated Pt wire (A); cyclic voltmetragrams (B) of AMI (50  $\mu\text{M}$ ) with scan rate 100  $\text{mV s}^{-1}$  under the pH 11 (a), 12 (b), and 13 (c); amperometric i-t curves (C) of AMI (50  $\mu\text{M}$  each step) under pH = 13 at platinum (a), copper (b), and Cu-Sn-Cr alloy modified (c) electrode. Electrolytes: 5 mM sodium acetate with

0.6 mM CTAB.

Figure 5. Electropherograms of the six AMGs under the different separation conditions: CTAB (A); pH (B); separation voltage (C). Other conditions were the same as in Figure 3. The peak of the analytes (50  $\mu$ M each): 1 = SPE, 2 = STR, 3 = AMI, 4 = KAN A, 5 = PAR, 6 = NEO.

Figure 6. Electropherograms corresponding to a mixture of standards (a), a spiking bovine serum sample (b), and the blank bovine serum sample (c). Other conditions were the same as in Figure 3. The peak of the analytes (50  $\mu$ M each): 1 = SPE, 2 = STR, 3 = AMI, 4 = KAN A, 5 = PAR, 6 = NEO.



**Figure 1.** The scheme and photography of the microfluidic chip. Channels: 50  $\mu\text{m}$  wide, 50  $\mu\text{m}$  deep. Injector (double-T) volume: 1.2 nL, separation channel: 57 mm, total length of Z-shape mixing channel: 2 mm, each double-T arms: 5 mm, each branch-like channel: 8 mm. Solution reservoirs: RB, running buffer reservoir; S, sample reservoir; SW, sample waste reservoir; BW, buffer waste reservoir; A1 / A2, alkaline reservoirs.

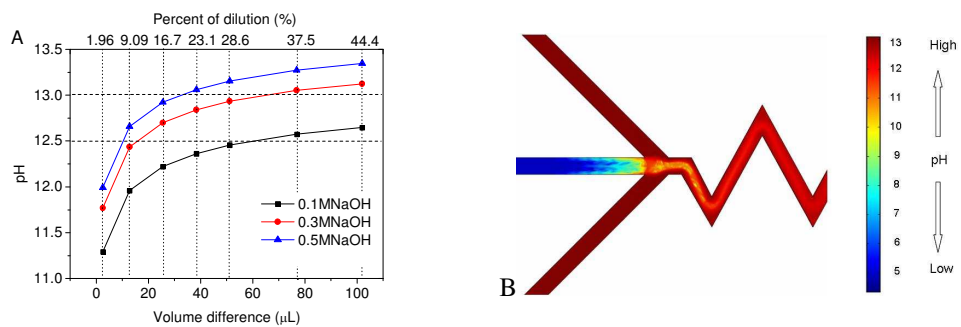


Figure 2. The plots (A) of the pH of the mixed solution vs. the volume difference (down x-axis) and the dilution percent of analytes (up x-axis); a computational simulation of the pH distribution in the mixing channel (B).

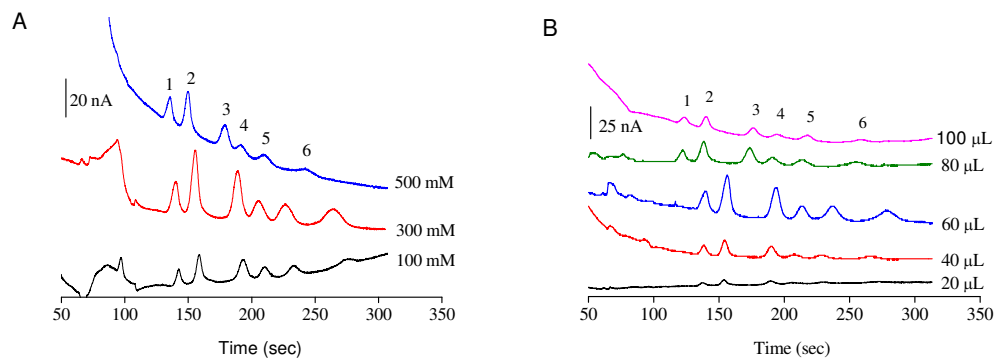


Figure 3. Electrophoregrams of AMGs under the post separation pH adjustment with the different concentration of NaOH at  $V_{(A-BW)} = 60 \mu\text{L}$  (A) and with the different  $V_{(A-BW)}$  at 0.3 M NaOH (B). Other conditions: running buffer 5 mM sodium acetate (pH = 4) with 0.6 mM CTAB, separation voltage – 1000 V, injection at -100 V / + 400 V for 10 s, detection potential = 0.65 V. The peak of the analytes (50  $\mu\text{M}$  each): 1 = SPE, 2 = STR, 3 = AMI, 4 = KAN A, 5 = PAR, 6 = NEO.

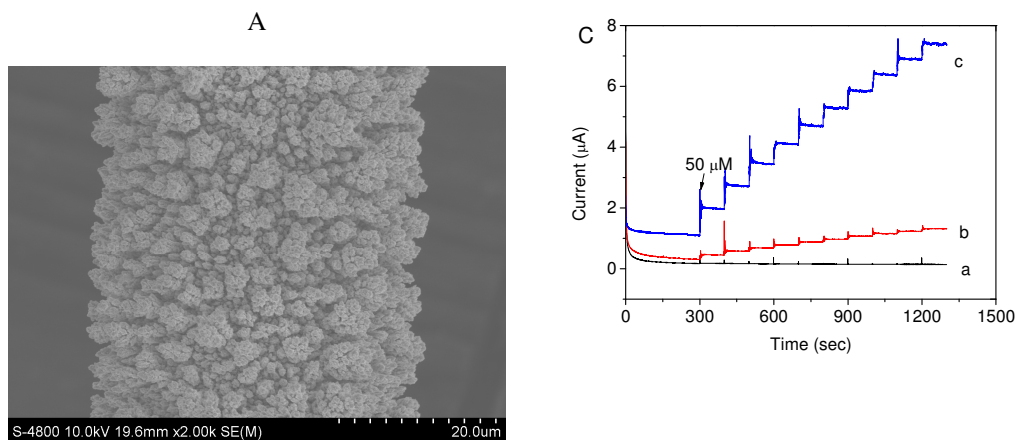


Figure 4. Characters of the alloy modified electrode: SEM of Cu-Sn-Cr alloy coated Pt wire (A); cyclic voltmetragrams (B) of AMI ( $50 \mu\text{M}$ ) with scan rate  $100 \text{ mV s}^{-1}$  under the pH 11 (a), 12 (b), and 13 (c); amperometric i-t curves (C) of AMI ( $50 \mu\text{M}$  each step) under pH = 13 at platinum (a), copper (b), and Cu-Sn-Cr alloy modified (c) electrode. Electrolytes: 5 mM sodium acetate with 0.6 mM CTAB.

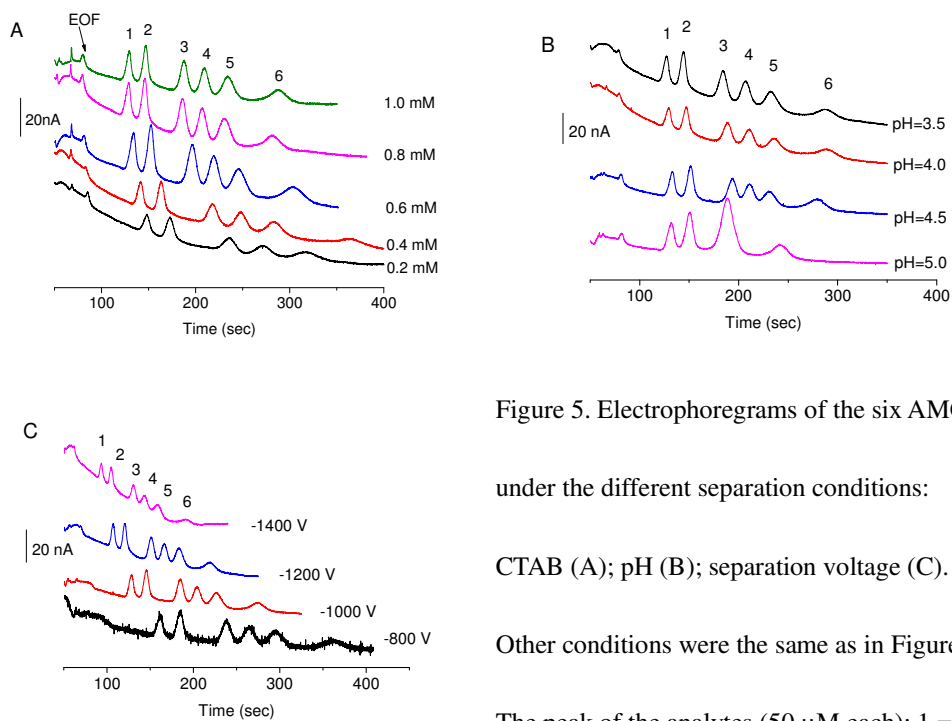


Figure 5. Electrophoregrams of the six AMGs

under the different separation conditions:

CTAB (A); pH (B); separation voltage (C).

Other conditions were the same as in Figure 3.

The peak of the analytes (50  $\mu$ M each): 1 =

SPE, 2 = STR, 3 = AMI, 4 = KAN A, 5 = PAR,

6 = NEO.

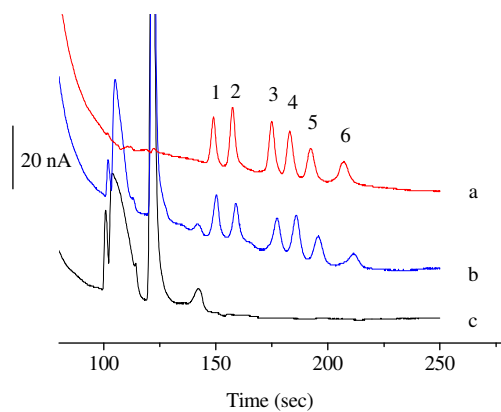
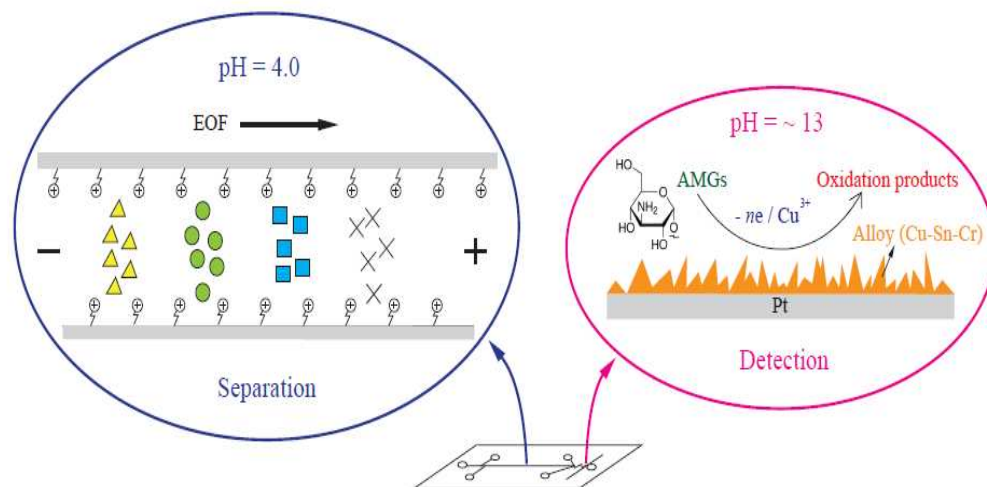


Figure 6. Electropherograms corresponding to a mixture of standards (a), a spiking bovine serum sample (b), and the blank bovine serum sample (c). Other conditions were the same as in Figure 3. The peak of the analytes ( $50 \mu\text{M}$  each): 1 = SPE, 2 = STR, 3 = AMI, 4 = KAN A, 5 = PAR, 6 = NEO.



A simple microfluidic technique was developed with the ability to adjust pH after separation for electrochemical detection of aminoglycoside antibiotics.